

Time-domain modelling of Extreme-Mass-Ratio Inspirals for the Laser Interferometer Space Antenna

Priscilla Canizares¹, and Carlos F. Sopuerta²

^{1,2} Institut de Ciències de l'Espai (CSIC-IEEC). Facultat de Ciències, Campus UAB, Torre C5 parells. Bellaterra, 08193 Barcelona, Spain.

E-mail: ¹ pcm@ieec.uab.es, ² sopuerta@ieec.uab.es

Abstract. When a stellar-mass compact object is captured by a supermassive black hole located in a galactic centre, the system loses energy and angular momentum by the emission of gravitational waves. Subsequently, the stellar compact object evolves inspiraling until plunging onto the massive black hole. These EMRI systems are expected to be one of the main sources of gravitational waves for the future space-based Laser Interferometer Space Antenna (LISA). However, the detection of EMRI signals will require of very accurate theoretical templates taking into account the gravitational self-force, which is the responsible of the stellar-compact object inspiral. Due to its potential applicability on EMRIs, the obtention of an efficient method to compute the scalar self-force acting on a point-like particle orbiting around a massive black hole is being object of increasing interest. We present here a review of our time-domain numerical technique to compute the self-force acting on a point-like particle and we show its suitability to deal with both circular and eccentric orbits.

1. Introduction

It is known that the majority of the galactic nuclei harbour a (super)massive black hole (MBH). Such a MBH can gravitationally capture a stellar-mass compact object (SCO), with mass in the range $m = 1 - 50M_{\odot}$, which eventually will perform a slow inspiral due to the emission of gravitational radiation until it plunges onto the MBH. These events are usually known as Extreme-Mass-Ratio Inspirals. EMRIs with MBHs with masses in the range $M = 10^4 - 10^7M_{\odot}$ are on the main targets of the future space-based gravitational-wave observatory LISA. One main issue is that EMRI signals will be buried in the LISA instrumental noise and the gravitational-wave foreground produced by compact galactic binaries inside the LISA band. In order to pull out these signals from the noise, we will have to cross-correlate the LISA data stream with a bank of EMRI waveform templates. These templates should be accurate enough to capture the physical relevant parameters of the system. For this reason, we need to include very precisely the gravitational *back-reaction* of the SCO on its own trajectory when modelling EMRIs. Due to the extreme mass ratios involved, an EMRI can be modeled within the framework of black hole perturbation theory, where the SCO is pictured as a point particle moving in the spacetime geometry of the MBH and the gravitational back reaction is described as the action of a local force, the *self-force*.

As a testbed for the development of numerical techniques to compute the self-force, we use a simplified EMRI system, in which the SCO is a scalar charged particle, with charge q , which orbits a non-rotating Schwarzschild MBH [1] and whose inspiral is driven by a self-force generated by

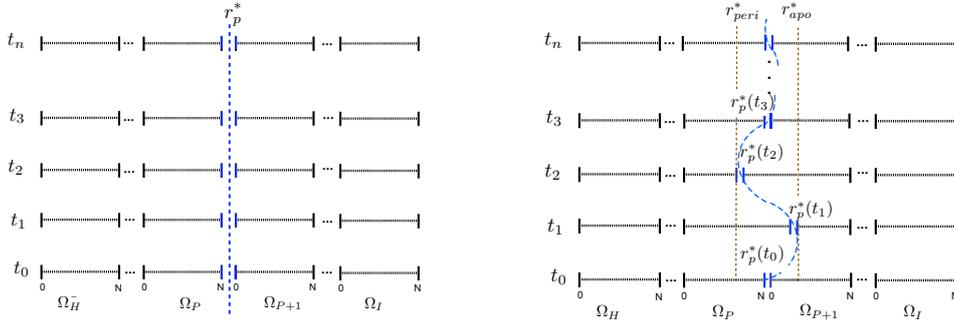


Figure 1. One-dimensional spatial grid for circular orbits (left) and eccentric orbits (right).

a scalar field, Φ . This simplified model contains all the essential ingredients of the gravitational problem. The scalar field Φ generated by the particle satisfies a wave equation in the MBH geometry, and the *scalar* self-force acting on the particle is given by: $F^\mu = q(g^{\mu\nu} + u^\mu u^\nu) (\nabla_\nu \Phi)|_\gamma$, where $u^\mu = dz^\mu/d\tau$ is the particle's velocity, and τ is proper time.

The spherical symmetry of the MBH spacetime implies that the retarded field can be decomposed into decoupled scalar spherical harmonics modes:

$$\Phi(x) = \sum_{\ell=0}^{\infty} \sum_{m=-\ell}^{\ell} \Phi^{\ell m}(t, r) Y^{\ell m}(\theta, \phi). \quad (1)$$

However, due to the singular character of the point particle, the sum over all the retarded field modes diverges at the particle location and, in order to obtain a self-force with a truly physical meaning, the field modes must be regularised. In order to do so, we use the *mode sum* regularisation scheme [2, 3, 4, 5, 6, 7], which gives an analytical expression for the singular contribution of the retarded field, Φ^S , at the particle location. Then, by subtracting the singular field modes from the retarded ones we obtain a smooth and differentiable field, $\Phi^R = \Phi - \Phi^S$, which generates the scalar self-force: $F^\mu = q(g^{\mu\alpha} + u^\mu u^\alpha) \nabla_\alpha \Phi^R$. Here, we review our work on the development of new techniques for the numerical computation of the retarded field, Φ . We also show the results we have obtained for the self-force after applying the mode-sum scheme.

2. Avoiding singularities: The Particle-without-Particle Formulation

In order to avoid the presence of the singularity associated with the point particle and all the related issues related with its numerical resolution we have proposed a new time-domain computational technique: *the Particle-without-Particle* (PwP) scheme. This technique was introduced in [8, 9] for the case of a charged scalar point particle orbiting in a circular orbit around a non-rotating MBH. In a subsequent work [10], the procedure was adapted to the case of eccentric orbits (see also [11]).

The main feature of our numerical scheme consists in splitting the one-dimensional spatial computational domain, parameterized in terms of the radial tortoise coordinate r^* , into two regions or subdomains, one at the left and one at the right of the particle: $r^* \in [-\infty, \infty] = [-\infty, r_p^*] \cup [r_p^*, \infty]$, where r_p^* denotes the particle radial location. Based on this division of the computational domain, all the variables associated with our problem can be written as: $\mathbf{U}(t, r^*) = \mathbf{U}_-(t, r^*) \Theta(r_p^*(t) - r^*) + \mathbf{U}_+(t, r^*) \Theta(r^* - r_p^*(t))$, where Θ is the Heaviside step function. In this way, by defining the jump of the variables as $[\mathbf{U}]_p \equiv \lim_{r^* \rightarrow r_p^*} \mathbf{U}_+(t, r^*) - \lim_{r^* \rightarrow r_p^*} \mathbf{U}_-(t, r^*)$

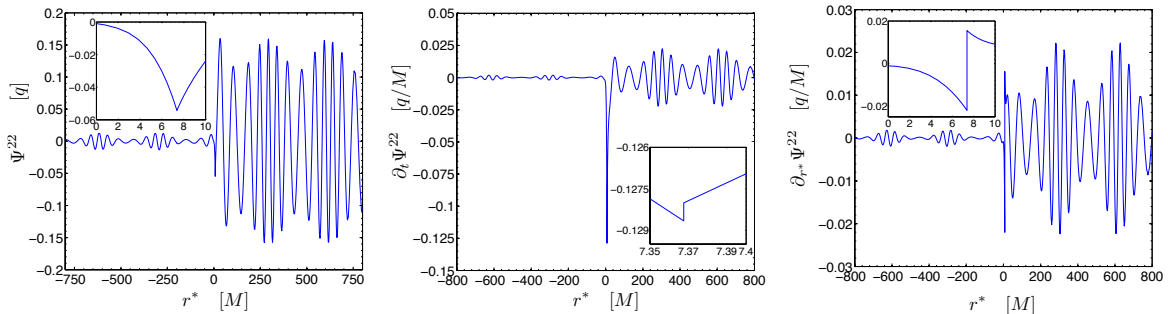


Figure 2. Snapshots of the evolution of the scalar field variable $\Psi = r \Phi$ (left), its time derivative $\partial_t \Psi$ (center), and its radial derivative $\partial_{r^*} \Psi$ (right), for a particle in an eccentric orbit with orbital parameters ($e = 0.2, p = 7M$). The internal frames show the ability of our method to resolve the different variables at the particle location, despite of the jumps in the time and radial derivatives. The snapshots have been taken after an evolution time $t_{\text{final}} - t_{\text{initial}} = 860M$.

(see [12, 9, 10]) we can obtain the jumps (matching conditions) at the particle location. Using this information we evolve the 1 + 1 wave-type equations for each mode inside each subdomain (which are homogeneous equations thanks to the PwP scheme). The solutions obtained are communicated through the boundaries by enforcing the analytic jumps. We have developed two practical methods for enforcing the jumps: (i) The *penalty* method, and (ii) the direct communication of the characteristic fields (see [10]). This is the essence of the PwP scheme, i.e. replacing the particle by a set of boundary conditions.

In our implementation of the PwP scheme, the spatial domain is discretized using the PseudoSpectral Collocation (PSC) method. In this way, each subdomain is discretized independently using a *Lobatto-Chebyshev* grid and the variables are expanded in a basis of Chebyshev polynomials (see [13, 9]). One of the most interesting properties of the PSC method is that it provides exponential convergence for smooth functions. The implementation for the circular case has no special difficulties as the particle is always at the same radial position (see Figure 1) and the domain structure is static and given by $\Omega = \bigcup_{a=1}^D \Omega_a$, where $\Omega_a = [r_{a,L}^*, r_{a,R}^*]$, and the particle is placed at the interface of two subdomains, say Ω_a and Ω_{a+1} , with $r_p^* = r_{a,R}^* = r_{a+1,L}^* = \text{const}$. However in the eccentric case, the radial position of the particle changes with time. In this case, we keep the particle at the interface by using a time-dependent mapping between the spectral domain, $[-1, 1]$, and the corresponding physical subdomains, so that the particle is always mapped to the boundaries of the spectral domain (see Figure 1).

3. Discussion

Here we have summarized our work on the development of new time-domain scheme for the computation of the self-force [9, 10], the PwP scheme. We have shown it is a suitable scheme by presenting results on the simplified case of a scalar point particle in circular and eccentric orbits around a non-rotating MBH. In Figure 2 we show snapshots of the evolution of the different variables used in our implementation both for circular and eccentric orbits. This figure shows that the computational scheme can resolve in a very smooth way the retarded field and its derivatives at the particle location. In particular it can resolve jumps in the derivatives of the scalar field, due to the particle (this is how the particle appears in our PwP scheme). Then, by applying the mode-sum regularization scheme we obtain the self-force components. In Table 1 we show the self-force results obtained for the particle in a circular orbit, ($e = 0.0, p = 6$), and also

Table 1. Self-Force components obtained for $\ell_{max} = 20$ and 24 subdomains

Circular Orbit Case (e = 0.0, p = 6 M)		
$\partial_t \Phi^R$	$\partial_r \Phi^R$	$\partial_\phi \Phi^R$
$3.608899 \cdot 10^{-4}$	$1.677117 \cdot 10^{-4}$	$-5.304114 \cdot 10^{-3}$
Eccentric Orbit Case (e = 0.2, p = 7 M)		
$\partial_t \Phi^R$	$\partial_r \Phi^R$	$\partial_\phi \Phi^R$
$4.278105 \cdot 10^{-4}$	$1.946249 \cdot 10^{-4}$	$-5.961118 \cdot 10^{-3}$

in a eccentric orbit with orbital parameters: ($e = 0.2, p = 7M$). In the circular case, the radial component of the self-force, the only one that needs to be regularized, agrees within a $1 \cdot 10^{-4}\%$ with the results obtained by [14] in the frequency domain. In Table 1 we also present results obtained for the eccentric orbit just mentioned. These results have been obtained by employing between 20 to 24 subdomains and 50 collocation points per domain. The average time for a full self-force calculation with $\ell_{max} = 20$ (which involves the calculation of 231 harmonic modes) in a computer with two Quad-Core Intel Xeon processors at 2.27GHz is around 10 to 15 minutes. See [11] for a detailed description of how to tune the method for performance and efficiency. In another recent work [15] we discussed the question of initial conditions and how to avoid the presence of spurious solutions that can affect self-force computations.

Acknowledgments

PCM is supported by a predoctoral FPU fellowship of the Spanish Ministry of Science and Innovation. CFS acknowledges support from the Ramón y Cajal Programme of the Ministry of Education and Science of Spain and by a Marie Curie International Reintegration Grant (MIRG-CT-2007-205005/PHY) of the European Community (FP7). We acknowledge the computational resources provided by the Centre de Supercomputació de Catalunya and the Centro de Supercomputación de Galicia (ICTS 121 and 175).

References

- [1] Poisson E 2004 *Living Rev. Relativity* **7** 6 (Preprint [gr-qc/0306052](#))
- [2] Barack L and Ori A 2000 *Phys. Rev.* **D61** 061502 (Preprint [gr-qc/9912010](#))
- [3] Barack L 2000 *Phys. Rev.* **D62** 084027 (Preprint [gr-qc/0005042](#))
- [4] Barack L 2001 *Phys. Rev.* **D64** 084021 (Preprint [gr-qc/0105040](#))
- [5] Barack L and Ori A 2002 *Phys. Rev.* **D66** 084022 (Preprint [gr-qc/0204093](#))
- [6] Detweiler S, Messaritaki E and Whiting B F 2003 *Phys. Rev.* **D67** 104016 (Preprint [gr-qc/0205079](#))
- [7] Haas R and Poisson E 2006 *Phys. Rev.* **D74** 044009 (Preprint [gr-qc/0605077](#))
- [8] Canizares P and Sopuerta C F 2009 *J. Phys. Conf. Ser.* **154** 012053 (Preprint [0811.0294](#))
- [9] Canizares P and Sopuerta C F 2009 *Phys. Rev.* **D79** 084020 (Preprint [0903.0505](#))
- [10] Canizares P, Sopuerta C F and Jaramillo J L 2010 *Phys. Rev.* **D82** 044023 (Preprint [1006.3201](#))
- [11] Canizares P and Sopuerta C F 2011 (Preprint [1101.2526](#))
- [12] Sopuerta C F and Laguna P 2006 *Phys. Rev.* **D73** 044028 (Preprint [gr-qc/0512028](#))
- [13] Boyd J P 2001 *Chebyshev and Fourier Spectral Methods* 2nd ed (New York: Dover)
- [14] Diaz-Rivera L M, Messaritaki E, Whiting B F and Detweiler S 2004 *Phys. Rev.* **D70** 124018 (Preprint [gr-qc/0410011](#))
- [15] Jaramillo J L, Sopuerta C F and Canizares P 2011 (Preprint [accepted 1101.2324](#))